

Supporting Information

Charge Transfer Dynamics in CsPbBr₃ Perovskite Quantum Dots- Anthraquinone/Fullerene (C₆₀) Hybrids

Sadananda Mandal*^a, Lijo George^a and Nikolai V. Tkachenko*^a

^aLaboratory of Chemistry and Bioengineering, Tampere University of Technology, P. O. Box 541, 33101 Tampere, Finland

Corresponding authors: E-mail: sadananda.mandal@tut.fi (S.M.); nikolai.tkachenko@tut.fi (N.V.T)

Materials and Methods

Materials

CsPbBr₃ PQDs and anthraquinone-2-carboxylic acid (AQ) were purchased from Sigma-Aldrich. The quantum dots are capped with oleyl amine and oleic acid and were dispersed in toluene. The PQDs with the emission wavelength of 510±5 nm were used in this study. According to the manufacturer, the diameter of the PQD is 9±0.5 nm and the emission quantum yield is 70%.

The synthesis of fullerene derivative (C₆₀) used in this study was described elsewhere.^{1,2} The PQD-AQ/C₆₀ hybrids were assembled using the fullerene and anthraquinone derivatives with carboxylic acid anchor. It is already reported by Zhu et al³ that the QD-organic hybrids with carboxylic acid functionalization are to be rather stable.

Sample Preparation

The supplied PQDs dispersed in toluene were diluted as required. The PQD-AQ/C₆₀ complexes were prepared by titration method. Microliter amount (maximum 20 µL) of AQ/C₆₀ solution was added into the PQD solution under vigorous stirring. Different ratios of PQD:AQ/C₆₀ (1:1 to 1:3) were prepared by adding different amount of AQ/ C₆₀ solution. The

optical density of PQD sample used in pump-probe measurement was roughly 0.45 at 470 nm wavelength in 2 mm cuvette.

Differential Pulse Voltammetry

The differential pulse voltammetry (DPV) technique was used to estimate the oxidation and reduction potentials of PQD, AQ and C₆₀ using a Ag/AgCl wire as a pseudoreference electrode. 0.1 M tetra-butylammonium hexafluorophosphate (TBAPF₆) in chloroform was used as the supporting electrolyte. After measuring the background, a chloroform solution of the sample was added to the electrochemical cell. To fix the reference potential, the measurements were repeated after adding ferrocene (in chloroform) solution for each sample. The measurements were carried out under a nitrogen flow in two directions: toward the positive and the negative potential. The final values of oxidation and reduction potentials were calculated as an average of the two scans relative to a ferrocene standard as reference.

Steady state absorption and emission

The UV-vis absorption spectra of PQDs and PQD-AQ/C₆₀ complexes were measured with a Shimadzu UV-3600 UV-vis-NIR spectrophotometer. The fluorescence emission spectra were recorded with an ISA-Jobin Yvon-SPEX-Horiba Fluorolog-3-111 fluorophotometer. The raw signals were corrected using an instrument response function provided by the manufacturer.

Time resolved single photon counting

The fluorescence lifetimes of the samples were measured using a time-correlated single photon counting (TCSPC) system by PicoQuant GmbH. The TCSPC system consists of a PicoHarp controller and a PDL-800B driver. The samples were excited by a pulsed laser diode (LDH-P-C-483) at 483 nm. The fluorescence decays were monitored at the emission maxima of PQD. The time resolution of the TCSPC system was approximately 120 ps.

Transient Absorption (TA) Spectroscopy

The TA spectroscopic measurements were carried out using a femtosecond pump-probe system. The details of instrumentation and methods were described in our previous publications.^{4,5} In brief, the samples were excited by laser pulses at the wavelength of 470 nm (Libra F, Coherent Inc., coupled with Topas C, Light Conversion Ltd.). A white continuum generator (sapphire crystal) was used to produce a probe beam. The TA responses were measured using an ExciPro TA spectrometer (CDP Inc.) equipped with a CCD array for the visible spectral range (490–750 nm), and an InGa diode array for the near-infrared wavelengths (895–1295). The pulse repetition rate of the laser system was 1 kHz and the

spectra were typically acquired by averaging over 5 s. Excitation energy was adjusted to avoid the effect of multiexciton generation (roughly 4 $\mu\text{J}/\text{cm}^2$).

Flash Photolysis

The transient absorption in the microseconds timescale was studied using the flash-photolysis method. The samples were excited by roughly 10 ns pulses at 470 nm produced by Ekspla NT342 laser system (Lithuania). A stabilized halogen light source (SLS201/M, Thorlabs, 9W) was used as the probe beam. The monochromatic (CM110, Digikröm) transient signal was detected with a silicon photoreceiver (2051-FS, New Focus) and recorded with a digitizing oscilloscope (TDS3032B, Tektronix, 300 MHz). A home-made program was used to control the experiment and average 100-1000 transient absorption responses to obtain desired signal-to-noise ratio. The measurements were carried out at a few wavelengths, and overall monitoring wavelength ranges were 500-950 nm and 550-1050 nm for PQD-AQ and PQD-C₆₀, respectively. The decays were fitted globally to multiexponential decay models using decfit program.

Decay model accounting for Poisson distribution of quenchers

To account for statistical formation of PQD-molecular acceptor hybrids a model assuming Poisson statistics of the complex formation was used. This model will be referred to as Poisson decay model and it predict the decay time profile to be⁶⁻⁸

$$f(t) = \exp\left\{-\frac{t}{\tau_0} - c\left[1 - \exp\left(-\frac{t}{\tau_q}\right)\right]\right\}$$

where τ_0 is the excited state lifetime of unquenched PQD, c is the relative concentration of the quencher, and τ_q is the quenching time constant in an ideal one-to-one PQD-acceptor complex. This model can also be used to account for the defect in PQDs.

Another decay model used in the global fit was so-called stretched-exponential:

$$f(t) = \exp\left[-\left(\frac{t}{\tau_s}\right)^\beta\right]$$

where τ_s is the time constant and β is the stretching parameter. Then the average time constant can be evaluated as

$$\tau_{av} = \frac{\tau_s}{\beta} \Gamma\left(\frac{1}{\beta}\right)$$

where $\Gamma\left(\frac{1}{\beta}\right)$ is the Gamma function.

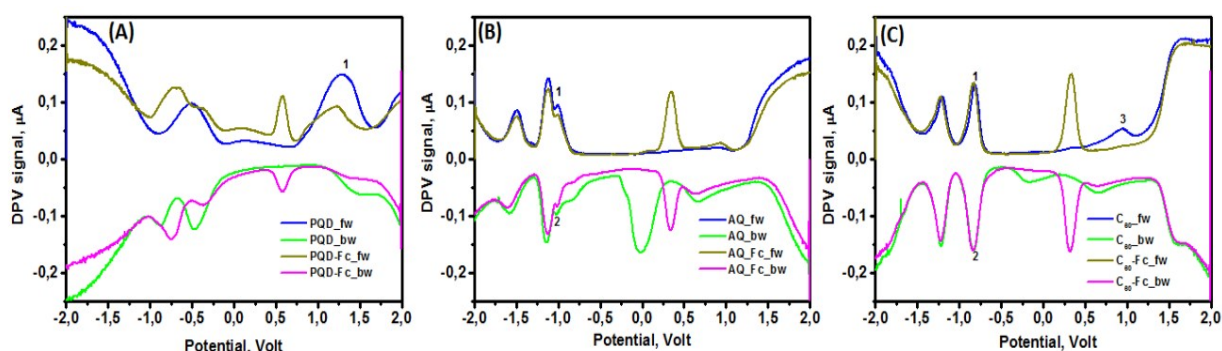


Figure S1. Differential pulse voltammogram of (A) PQD, (B) AQ and (C) C₆₀: bg-background, fw-forward scan, bw-backward scan, Fc-ferrocene

DPV data Analysis

Calculation of VB, CB, HOMO, LUMO energy of PQD, AQ and C₆₀

	Reduction, V	Oxidation, V
AQ vs. AgAgCl	- 0.99	
Fc/Fc+ vs. AgAgCl		+0.35
AQ vs. Fc/Fc+	- 1.34	
Fc/Fc+ vs. vacuum		-4.80
AQ vs. vacuum	- 3.46	
	LUMO, eV	HOMO, eV

	Reduction, V	Oxidation, V
C ₆₀ vs. AgAgCl	- 0.82	+ 0.94
Fc/Fc+ vs. AgAgCl		+ 0.34
C ₆₀ vs. Fc/Fc+	- 1.16	+ 0.60
Fc/Fc+ vs. vacuum		- 4.80
C₆₀ vs. vacuum	- 3.64	- 5.40
	LUMO, eV	HOMO, eV

	Reduction, V	Oxidation, V
PQD vs. AgAgCl	- 0.51	+ 1.28
Fc/Fc+ vs. AgAgCl		+ 0.58
PQD vs. Fc/Fc+	-1.09	+ 0.70
Fc/Fc+ vs. vacuum		- 4.80
PQD vs. vacuum	- 3.00	- 5.50
	CB, eV	VB, eV

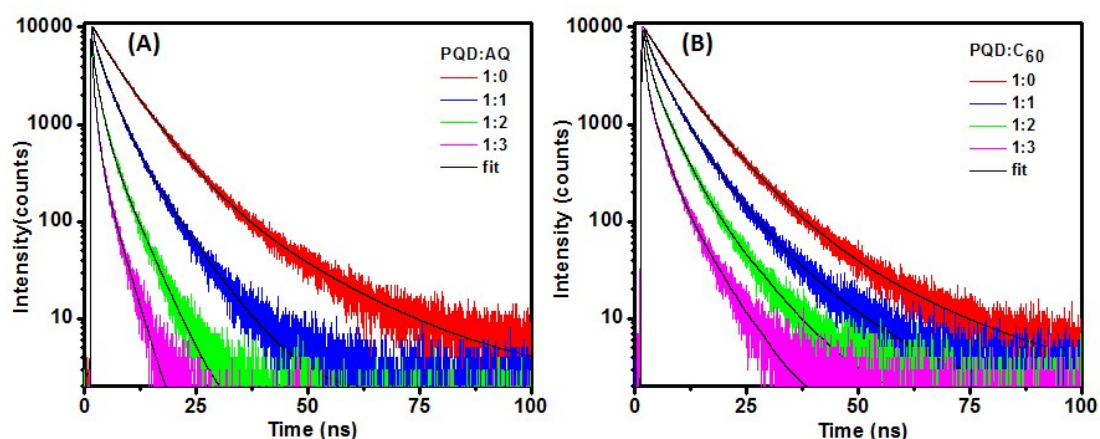


Figure S2. Emission decays of (A) PQD-AQ and (B) PQD-C₆₀ at the excitation wavelength of 483 nm and monitoring wavelength of 510 nm.

Table S1 Emission decay parameters of PQD and PQD-AQ, the time constants, τ_i , corresponding pre-exponential factors, a_i , and the average lifetime, $\langle\tau\rangle$

PQD: AQ	τ_1 , ns (a_1)	τ_2 , ns (a_2)	τ_3 , ns (a_3)	$\langle\tau\rangle$, ns
1:0	4.08 (0.38)	7.74 (0.59)	20.62 (0.03)	6.64
1:1	0.34 (0.42)	2.88 (0.47)	6.9 (0.11)	2.28
1:2	0.17 (0.67)	1.36 (0.26)	4.14 (0.07)	0.76
1:3	0.11 (0.78)	0.73 (0.19)	2.69 (0.03)	0.31

Table S2 Emission decay parameters of PQD and PQD-C₆₀, the time constants, τ_i , corresponding pre-exponential factors, a_i , and the average lifetime, $\langle\tau\rangle$

PQD: C ₆₀	τ_1 , ns (a_1)	τ_2 , ns (a_2)	τ_3 , ns (a_3)	$\langle\tau\rangle$, ns
1:0	4.08 (0.38)	7.74 (0.59)	20.62 (0.03)	6.64
1:1	1.53 (0.39)	4.95 (0.56)	11.67 (0.05)	3.95
1:2	0.87 (0.59)	3.6 (0.36)	8.39 (0.05)	2.20
1:3	0.48 (0.73)	2.30 (0.22)	5.66 (0.05)	1.11

Re-evaluation of the PQD:AQ/C₆₀ ratios based on emission quenching by Poisson statistics

At concentrations used in this study ($<10 \mu\text{M}$) one can neglect by diffusion controlled processes, and assume that only ground state complexes will show emission intensity and lifetime quenching. For the quantitative estimation of the degree of quenching Poisson statistics of the complex formation was used.⁶ In a very rough approximation one can assume that only PQD which did not form a complex emit light, but PQD with one and more acceptors do not emit light at all. In a more accurate approach one need to account separately for the emission efficiency in complexes with different number of acceptors by assuming that lifetime of the excited state of PQD alone is τ_0 , quenching time constant is τ_{ET} and thus quenching efficiency in 1:1 complex is τ_{ET}/τ_0 , in 1:2 complex is $\tau_{ET}/2\tau_0$, and so on, if $\tau_0 \gg \tau_{ET}$. This model can be used to approximate concentration quenching dependence of both series of samples, PQD-AQ and PQD-C₆₀, by scaling relative concentration of the acceptor as shown in Figure S3, where average values $\tau_0 = 6.6 \text{ ns}$, $\tau_{ET} = 0.16 \text{ ns}$ were used. These results show that the scaling factor for PQD-AQ 0.95 which is equal to unity within experimental accuracy, and indicates stable ground state complex formation. For PQD-C₆₀ samples the

scaling factor is 0.80 which is lower than one a small margin. One can also notice rather big difference in quenching efficiency for different series of PQD- C_{60} samples. The difference may arise from a poor solubility of C_{60} and some loss of the material during injection process.

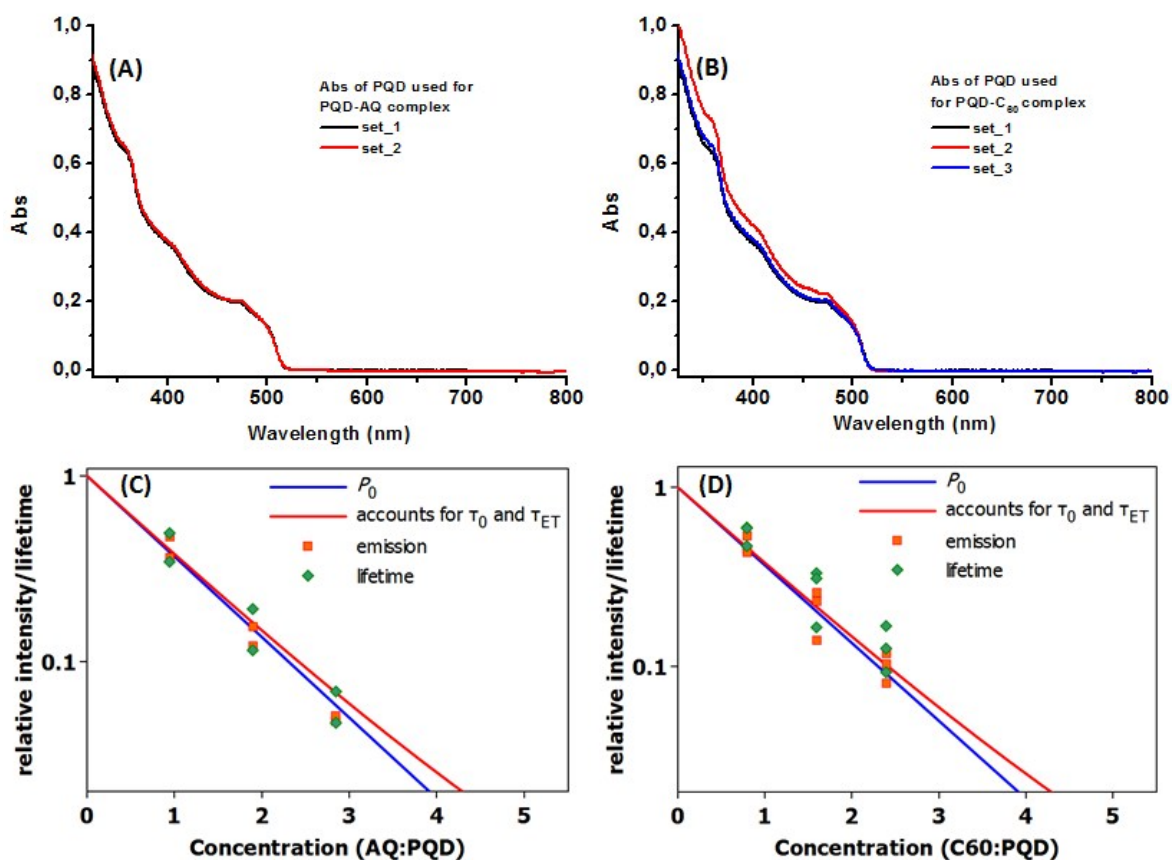


Figure S3. Absorption spectra of PQD used for complex formation with (A) AQ and (B) C_{60} . Steady state emission and emission decay data scaled by PQD:AQ(C_{60})= 1:0.95(0.80) and presuming $\tau_0 \gg \tau_{ET}$ (P_0 , blue line) and taking $\tau_0 = 6.6$ ns, $\tau_{ET} = 0.16$ ns (red line, τ_0 is the lifetime of a nonhybridized PQD and τ_{ET} is the electron transfer time constant), (C) AQ:PQD and (D) C_{60} :PQD.

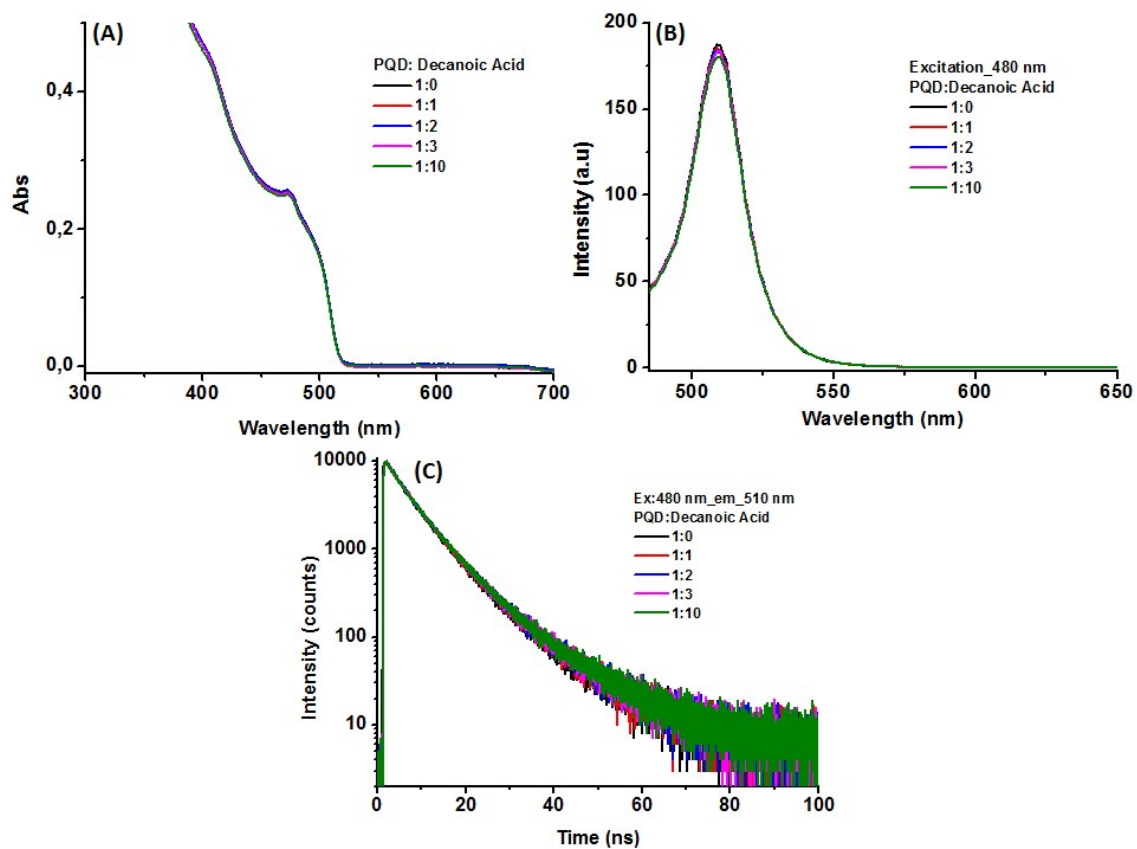


Figure S4: Steady state (A) absorption, (B) emission spectra and (C) emission decay curves of PQD and different ratios of PQD:Decanoic Acid.

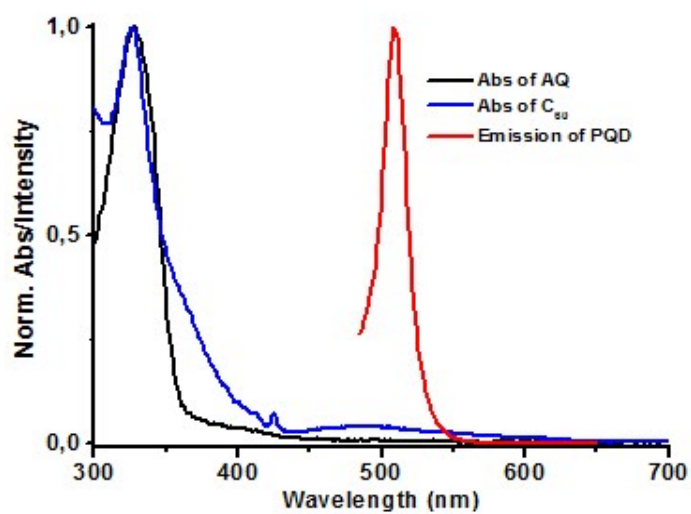


Figure S5. Normalized absorption spectra of AQ and C₆₀ and emission spectrum of PQD.

Transient absorption spectroscopy

The excitation density dependence of PQDs TA responses was studied by changing the average excitation power as shown in the Figure S6. An estimated excitation spot size was 1 mm and excitation repetition rate was 1 kHz, thus 10 μW corresponds to roughly 1.3 $\mu\text{J}/\text{cm}^2$ and 270 μW to 36 $\mu\text{J}/\text{cm}^2$. Since the normalized TA response at the excitation average power 30 μW (or roughly 4 $\mu\text{J}/\text{cm}^2$) was virtually identical to the response at three times lower density, we concluded that there is no bi-exciton effects at excitation power upto 30 μW and used this power for further TA measurements.

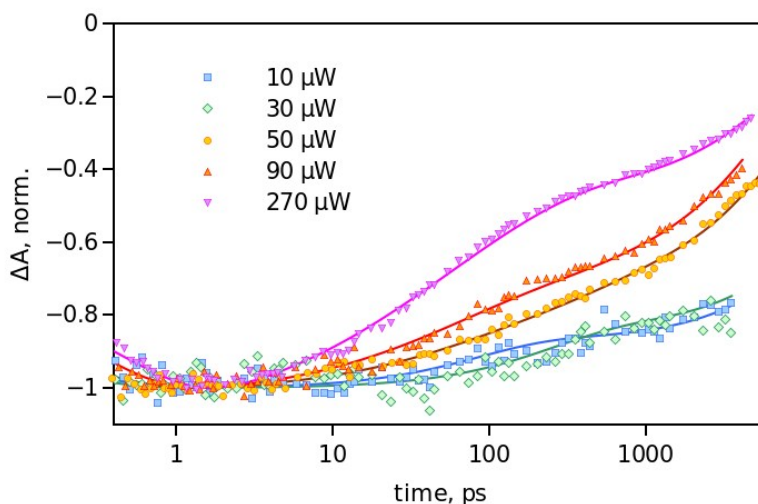


Figure S6: Recovery of the ground state bleaching at 504 nm of PQD sample excited at 470 nm with different excitation density measured as the average excitation power. The transient responses are normalized for the comparison purpose. The time scale is logarithmic.

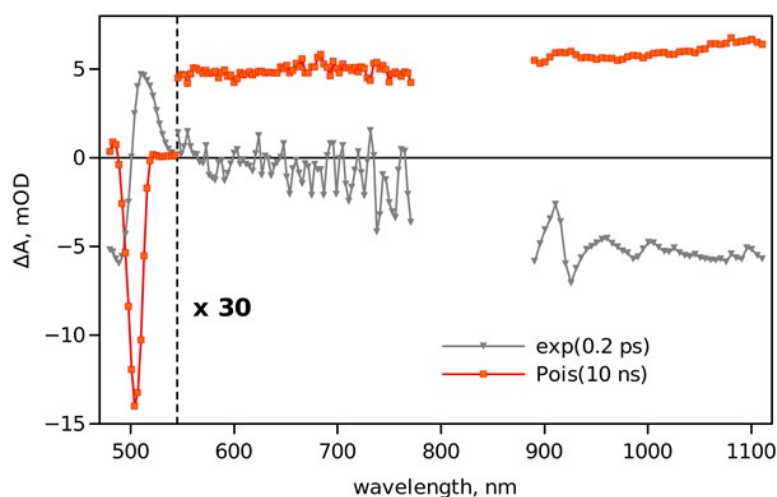


Figure S7: Transient absorption decay component spectra of PQD after global fitting. The fit model consisted of a fast exponential decay (0.2 ps) attributed to hot carrier thermalization, and a decay accounting for a Poission defect distribution which gives $\tau_0 = 10$ ns (longer than

the measurement time scale) quenching time constant of roughly 150 ps and relative concentration of the defects 23%.

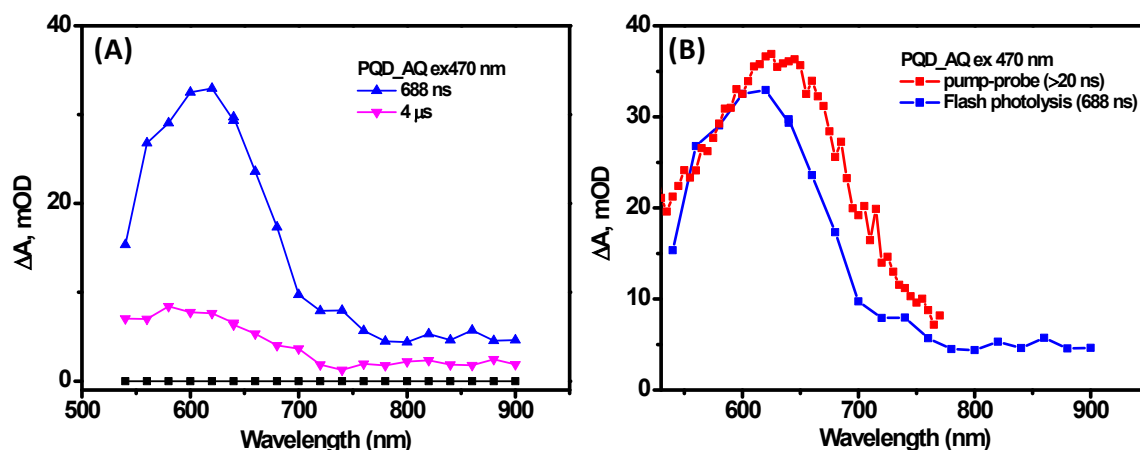


Figure S8. (A) Decay component spectra of PQD-AQ hybrid measured by flash photolysis after global fitting, (B) Comparable spectra measured by pump-probe and flash photolysis.

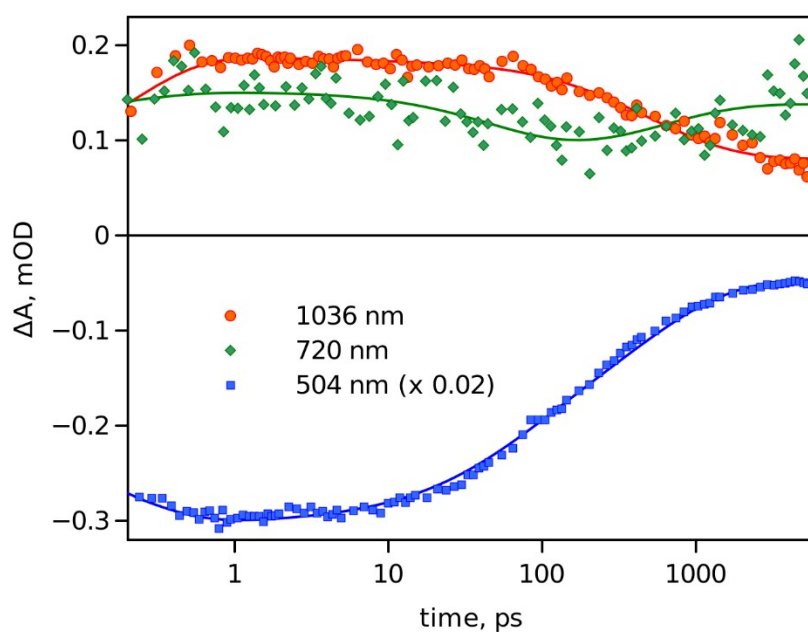


Figure S9: Transient absorption decay profiles of PQD-C₆₀ at three selected wavelengths (indicated on the plot). Symbols are measured data and solid lines are global fits. Decay at 504 nm is multiplied by 0.02 to fit the scale. Time scale is logarithmic. Note: Noticeably, the decay at 504 nm becomes visible at few tens picosecond delay time but only at few hundreds delay time at 1036 nm, which can be attributed to roughly the same absorption of PQD excited state and C₆₀ anion at this wavelength. Secondly, the response at 720 nm is noisy but an increase in the absorption is visible at delay approaching 1 ns and longer, when the remaining bleaching at 504 nm is at the level of one quarter and it continue to decline, which means that the absorption band at 720 nm is not related to PQDs.

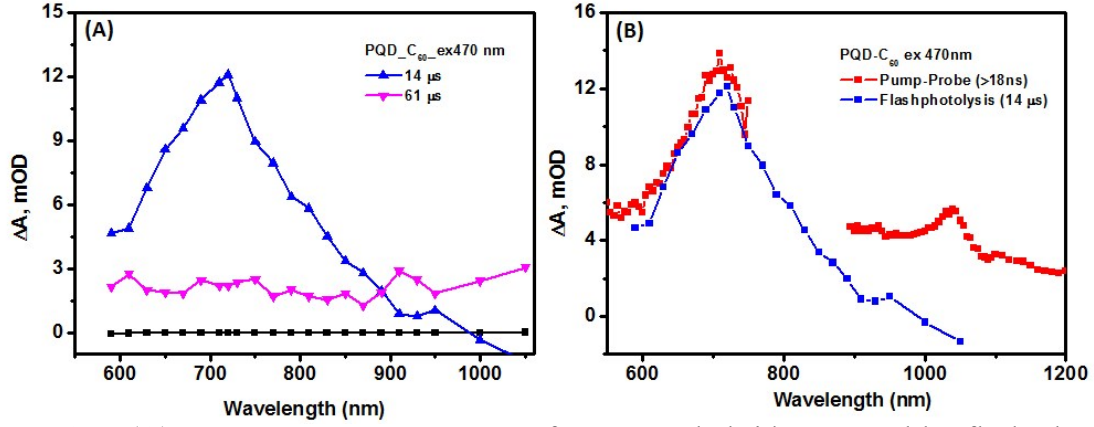


Figure S10. (A) Decay component spectra of PQD-C₆₀ hybrid measured by flash photolysis after global fitting, (B) Comparable spectra measured by pump-probe and flash photolysis.

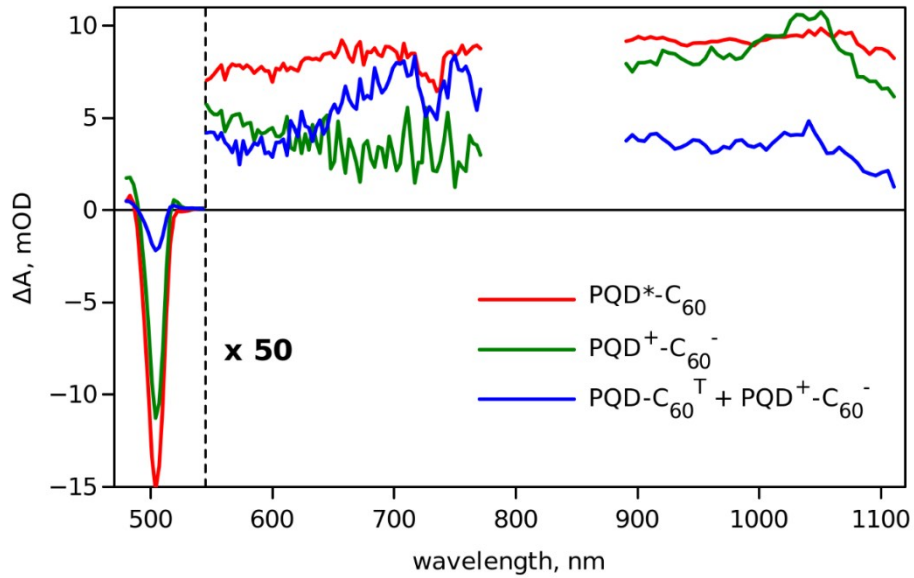


Figure S11. Differential spectra of intermediate states of PQD-C₆₀ hybrid

Estimation of reorganization energy and electronic coupling

According to semi-quantum Marcus ET theory, the rate constant of the electron transfer is ⁹⁻¹¹

$$k_{ET} = \frac{2\pi^{3/2}V^2}{h\sqrt{\lambda k_B T}} \sum_{i=0}^{\infty} e^{-S} \frac{S^i}{i!} \exp\left[-\frac{(\Delta G_0 + \lambda + ih\nu_{vib})^2}{4\lambda k_B T}\right]$$

where k_B is the Boltzmann constant, V is the electronic coupling, ΔG_0 is the reaction free energy, $h\nu_{vib}$ is the energy of the fundamental vibrational mode, S is the electronic-vibrational coupling, and λ is the outersphere reorganization energy. The latter can be evaluated in frame of the continuum model ¹¹

$$\lambda = \frac{q_e^2}{4\pi\epsilon_0} \left(\frac{1}{2R_D} + \frac{1}{2R_A} - \frac{1}{R_{DA}} \right) \left(\frac{1}{\epsilon_{opt}} - \frac{1}{\epsilon_s} \right)$$

where q_e is the electron charge, ϵ_{opt} and ϵ_s are the optical and static dielectric constants, R_A and R_D are the radii of the acceptor and donor and R_{DA} is the donor-acceptor center to center distance. Due to rather large size of the PQD, and relatively small size of acceptors the reorganization energy is small and depends weakly on the acceptor size and donor-acceptor distance (which does not differ much for the acceptors used), and can be evaluated to be $\lambda = 0.14 - 0.16$ eV. ΔG_0 was estimated for both charge separation and charge recombination reactions (see Fig. 6 in the main text), a reasonable value of $h\nu_{vib}$ is 0.25 eV.⁹ Thus, we have two rate constants (CS and CR reactions) and two unknown parameters, V and S . There is no analytical solution to the problem, but a fit suggests $V = 0.7$ meV (or 6 cm^{-1}) and $S = 1.2$, or internal reorganization energy for PQD-AQ to be 0.3 eV, which is a reasonable value for anthraquinone reorganization in transitioning between anion and neutral states (it also suggests that PQD internal reorganization is much smaller). For PQD-C₆₀ hybrid similar estimation cannot be carried out as the CS state relaxes to the triplet state.

References

- (1) Stranius, K.; George, L.; Efimov, A.; Ruoko, T.-P.; Pohjola, J.; Tkachenko, N. V. *Langmuir* **2015**, *31* (3), 944–952.
- (2) Nierengarten, J.-F.; Herrmann, A.; Tykwinski, R. R.; Riittimann, M.; Diederich, F.; Boudon, C.; Gisselbrecht, J.-P.; Gross, M. *Helv. Chim. Acta* **2004**, *80* (1), 293–316.
- (3) Zhu, H.; Song, N.; Lian, T. *J. Am. Chem. Soc.* **2010**, *132* (42), 15038–15045.
- (4) Virkki, K.; Demir, S.; Lemmetyinen, H.; Tkachenko, N. V. *J. Phys. Chem. C* **2015**, *119* (31), 17561–17572.
- (5) Virkki, K.; Hakola, H.; Urbani, M.; Tejerina, L.; Ince, M.; Martínez-Díaz, M. V.; Torres, T.; Golovanova, V.; Golovanov, V.; Tkachenko, N. V. *J. Phys. Chem. C* **2017**, *121* (17), 9594–9605.
- (6) Sadhu, S.; Tachiya, M.; Patra, A. *J. Phys. Chem. C* **2009**, *113* (45), 19488–19492.
- (7) Tkachenko, N. V. *ChemPhotoChem* **2018**, *2*, 112-120.
- (8) Mandal, S.; Iglesias, M.G.; Ince, M.; Torres, T.; Tkachenko, N.V. *ACS Omega* **2018**, *3*, 10048–10057
- (9) Pla, S.; Niemi, M.; Martin-Gomis, L., et al, *Phy.Chem.Chem.Phys*, **2016**, *18*, 3598-3605.
- (10) Barbara, P. F.; Meyer, T. J.; Ratner, M. A., *J. Phys. Chem.*, **1996**, *100*, 13148-13168.
- (11) Bolton, J. R.; Archer, M. D., *Adv. Chem. Ser.*, **1991**, *228*, 7-23.